Design of broadband and dual-band microstrip antennas on a high-dielectric substrate using a genetic algorithm

H. Choo and H. Ling

Abstract: The authors report the use of a genetic algorithm (GA) to design patch shapes for microstrip antennas on a high-dielectric substrate for broadband and dual-band applications. A full-wave electromagnetic solver is employed to predict the performance of microstrip antennas with arbitrary patch shapes. A two-dimensional chromosome is used to encode each patch shape into a binary map. A GA with a two-point crossover and geometrical filtering is implemented to achieve efficient optimisation. The resulting optimised patch structures for broadband and dual-band operations are described. For broadband application, the optimised patch antenna achieves a four-fold improvement in bandwidth when compared to a standard square microstrip antenna. For dual-band application, the optimised patch antenna shows a good impedance match at the design frequencies of 1 and 2 GHz. The GA-optimised designs are built on a FR-4 substrate and measurement results show good agreement with the numerical prediction. Physical interpretation for the optimised shapes is discussed.

1 Introduction

It is well known that microstrip antennas have an intrinsically narrow bandwidth. Much research has been carried out to improve the bandwidth of microstrips, and a number of different techniques have been published, including adding parasite patches, adopting multi-layer structures, using a thick air substrate, and adding a shorting post as reactive loading [1, 2]. However, these techniques are usually accompanied by an increase in overall size or manufacturing cost. In the past few years, many researchers have applied genetic algorithms (GA) to the design of electromagnetic systems [3]. A two-dimensional (2-D) microstrip shape design was reported in [4, 5]. Alatan *et al.* [4] employed a GA to design circularly polarised (CP) microstrip antennas by optimising the corners of a square microstrip. Johnson and Rahmat-Samii [5] showed that it is possible to obtain novel shapes for broadband and dual-band applications by using a GA. They used air as the substrate material by suspending a patch above the ground plane. The attractiveness of GA shape optimisation is that improved performance can be achieved without increasing the overall volume or manufacturing cost.

In this paper, we also examine the use of a GA for broadband and dual-band applications. In contrast to the work of Johnson and Rahmat-Samii, we employ standard FR-4 as the substrate, since it is the most commonly used material in wireless devices. A microstrip built on a high-dielectric-material substrate such as FR-4 (dielectric constant of 4.3) has a narrower bandwidth. Consequently, it is more challenging to obtain the desired frequency characteristics without sufficient degrees of freedom in the design process. In our approach, we employ a full-wave electromagnetic (EM) patch code to predict the performance of an arbitrary shaped microstrip. A GA algorithm is implemented to optimise the patch shape that is encoded into a 2-D chromosome. A 2-point crossover scheme with three chromosomes is used as a crossover operator to achieve faster convergence. In addition, geometrical filtering is adopted to create more realisable shapes. We first apply this methodology to a broadband patch antenna design (some preliminary results were presented earlier in [6]), and then we apply a GA to a dual-band patch design.

2 GA optimisation

To predict the performance of each patch shape, we use an electromagnetic simulation code adapted from a code for analysing frequency selective surfaces [7, 8]. The code uses the electric field integral equation (EFIE) formulation in conjunction with the periodic Green's function for a layered medium. Rooftop functions are used as basis functions to represent the currents on the patch. To speed up the computation of the matrix elements, the fast Fourier transform (FFT) is employed. To further reduce the matrix fill time during the GA, the matrix elements for all the possible basis positions are computed and stored before the GA process. Consequently, the moment matrix for any patch shape can be easily assembled without any computation.

To achieve broadband and dual-band operations, we implement the GA as an optimiser for the microstrip patch shape. The algorithm starts with an initial population of shapes that are encoded as chromosomes. After these chromosomes are evaluated by the EM simulation code, a cost function is computed. According to the cost function, the chromosomes are refined into the next generation through a reproduction process including crossover,

IEE Proceedings online no. 20030291

doi:10.1049/ip-map:20030291

Paper first received 20th February and in revised form 14th October 2002

The authors are with the Department of Electrical and Computer Engineering, The University of Texas at Austin, Austin, TX78712-1024, USA

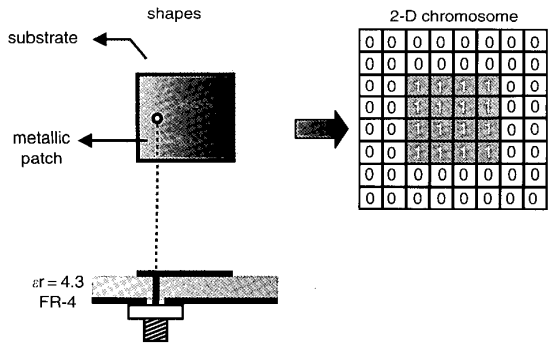

Fig. 1 *2-D encoding of patch shapes for broadband shape optimisation*

mutation and geometrical filtering. This series of processes is repeated until the cost function is minimised.

In our GA, we represent each patch shape as a binary bitmap. In the resulting two-dimensional (2-D) chromosome [9], ones represent the metallised areas and zeros represent the areas without metal (Fig. 1). Since it is more desirable to have a well-congregated patch shape in the final design, we apply a 2-D median filter [10] to the chromosomes at each generation of the GA process. Fig. 2 shows a sample chromosome before and after the 2-D median filter operation. Before median filtering, the chromosome shows many isolated patches. After median filtering, most of the isolated patches in the chromosome are gone, and the overall shape of the chromosome becomes more gathered. For the crossover operation, a 2-point crossover scheme using three chromosomes is used to boost the GA convergence rate. This more disruptive crossover scheme counteracts against the median filtering effect and shows a better convergence rate.

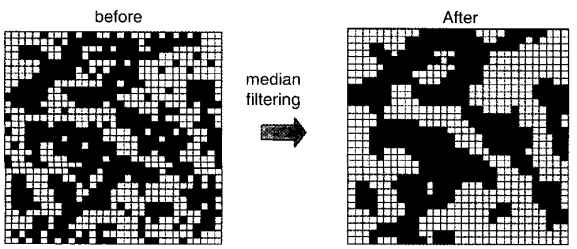

Fig. 2 *Median filtering*

3 Broadband microstrip antenna design

3.1 GA optimisation for broadband application

In this Section, our design goal is to broaden the bandwidth of a microstrip by exploring arbitrary patch shapes through a GA. To achieve the design goal, we define a cost function as

$$Cost = \frac{1}{N}\sum_{n=1}^{N} P_n \qquad (1)$$

where

$$P_n = \begin{cases} S_{11}(\text{dB}) + 10\,\text{dB} & \text{if } S_{11}(\text{dB}) \geq -10\,\text{dB} \\ 0 & \text{if } S_{11}(\text{dB}) < -10\,\text{dB} \end{cases}$$

The cost function in (1) averages those S_{11} values (in dB) that exceed -10 dB within the desired frequency range. In the GA process, the cost function is an important factor not only for the final design but also for the overall GA convergence time. To reduce the computational burden, an adaptive cost function is used. In the first stage of the GA process, we use a small frequency range compared to the eventual design goal, then we gradually increase the frequency range whenever the cost converges to a minimum. This process is repeated until the eventual design goal is achieved. In general, the number of frequency calculations required in this scheme is much less than if the entire design frequency band is used throughout the GA iterations.

In our GA, the size of the population is 30. A crossover probability of 80% is used, while the probability of mutation is set to 10%. The frequency range is set between 1.9 GHz and 2.1 GHz. We use a square design area (72 mm × 72 mm) and an FR-4 substrate with a thickness of 1.6 mm. The design area is discretised into a 40 × 40 grid. Fig. 3 is the resulting shape of the GA-optimised microstrip. The white dot represents the location of the probe feed. Note that the position of the feed is one of the parameters to be optimised, since the patch has the freedom to reside anywhere within the total design area. The total time of the design process is about 24 h on ten Pentium III (550 MHz) machines running in parallel. For experimental verification, we built a prototype of the GA-optimised microstrip patch using aluminum tape (copper tape was also tried with nearly identical results). A photo of the tested patch is shown in Fig. 4. Fig. 5 shows the return loss comparison between the measurement and the simulation results. Good agreement is observed. The bandwidth is found to be 8.5% by simulation and 8.1% by measurement. We should point out that we have earlier applied the same GA methodology under a coarser 16 × 16 grid and a 32 × 32 grid within the same design area [6]. As we increased the design resolution of the grid from 16 × 16 to 32 × 32, the bandwidth was improved by about 30%. However, the higher resolution 40 × 40 grid shows only a slight bandwidth increment compared to that of the 32 × 32 grid. We have also measured the gain of the GA-optimised microstrip relative to the reference square

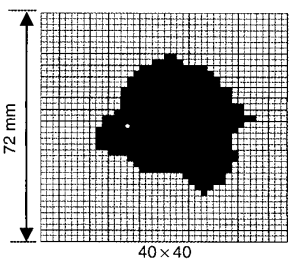

Fig. 3 *The GA-optimised microstrip antenna using 40 × 40 resolution within a 72 mm × 72 mm area. The grey pixels are metal and the white dot shows the position of the probe feed*

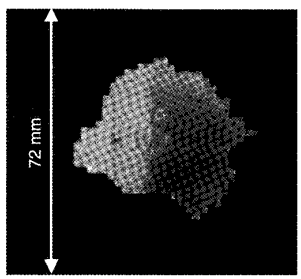

Fig. 4 *A picture of the microstrip antenna built on FR-4 circuit board*

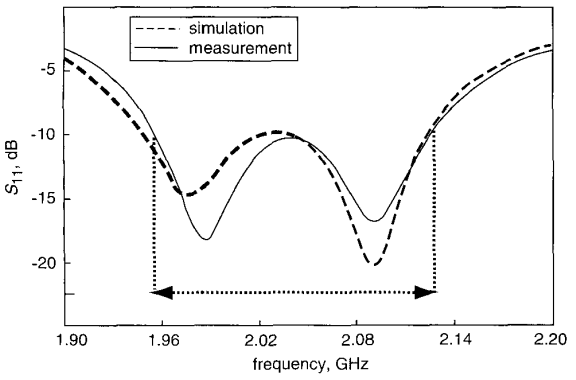

Fig. 5 *Return loss (dB) of the GA-optimised antenna from simulation and measurement*

microstrip under the same construction. A nearly negligible gain loss is observed (0.9 dB gain loss at 1.98 GHz, and 1.0 dB at 2.1 GHz).

3.2 Operating principle of the GA design

We now try to provide an interpretation of the operating principle of the GA-designed antenna. The two frequency dips in Fig. 5 show that the antenna supports two operating modes very close to each other in frequency. To verify the two operating modes, we analyse the current distributions on the patch around these frequencies. Figs. 6*a* and *b* show the current plots at 1.98 GHz and 2.1 GHz, respectively. At 1.98 GHz, current flows predominantly in the downward-right direction, whereas at 2.1 GHz, current flows predominantly in the upward-right direction. The currents corresponding to the two modes are nearly perpendicular to each other. The two-mode operation can be seen even more clearly in the measured radiation pattern plots. Figs. 7*a* and *b* show the radiation patterns at the two frequencies along the two dashed cuts. We observe that at 1.98 GHz the dominant polarisation is in the $\phi = -45°$ plane, whereas at 2.1 GHz the dominant polarisation is in the $\phi = 45°$ plane, as we would expect from the current plots. This two-mode operation improves the bandwidth of a square microstrip by a factor of about three. Note that the enhancement of the bandwidth in this antenna comes at the price of polarisation purity, which was not a constraint in our GA process. For some applications where the depolarisation from the propagation channel is dominant, polarisation purity might not be a strong design consideration.

We also observe an additional important bandwidth enhancement effect through the ragged edge shape. When we restricted the patch to have a single-mode operation by

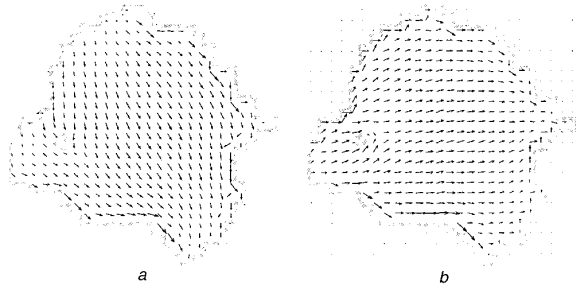

Fig. 6 *Current distribution on the surface of GA-optimised patchs*
a At 1.98 GHz
b At 2.1 GHz

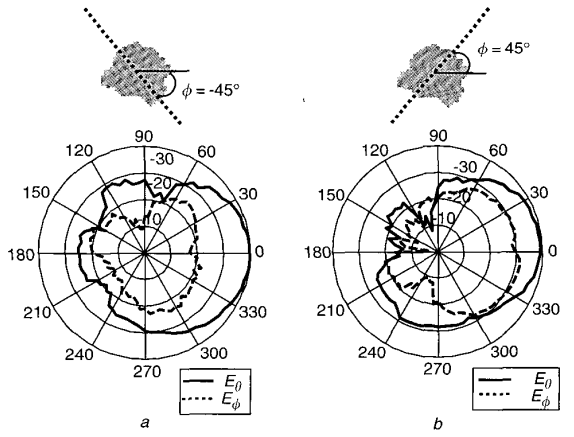

Fig. 7 *Measured radiation patterns*
a At 1.98 GHz ($\phi = -45°$ plane)
b At 2.1 GHz ($\phi = 45°$ plane)

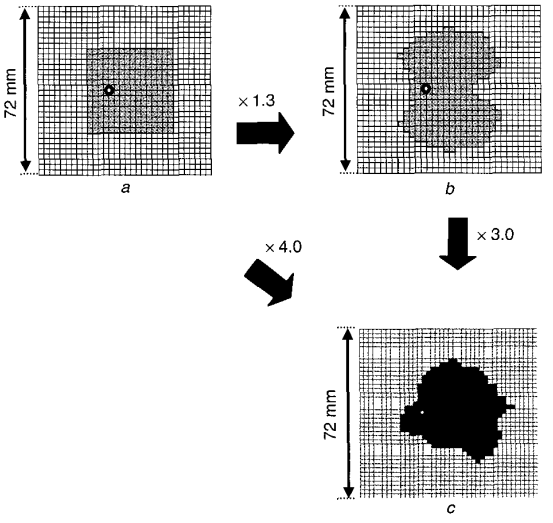

Fig. 8 *Bandwidth enhancement achieved by two-mode operation and ragged edges*

symmetry constraints, the ragged edges in the GA-optimised shape enhanced the bandwidth by about 30% compared to the reference square microstrip. This is shown in Figs. 8*a* and 8*b*. We believe the ragged edges cause the broadening of the resonant frequency by introducing multiple resonant lengths between the two radiating edges on the two sides of the patch. Therefore this ragged edge shape, in conjunction with the two-mode operation in our GA-optimised design in Fig. 8*c*, results in the broadest bandwidth possible (× 4.0 compared to Fig. 8*a*).

4 Miniaturised dual-band microstrip antenna design

4.1 GA and cost function for dual-band design

We now apply GA to the design of a dual-band microstrip. The same substrate material and substrate thickness as in the broadband design are used. Our design goal is to produce a good impedance match at frequencies of 1 and 2 GHz. In addition, we put a constraint on the size of the patch to be 42.5 mm × 40 mm. This patch size is 40% smaller than that of a standard square microstrip working

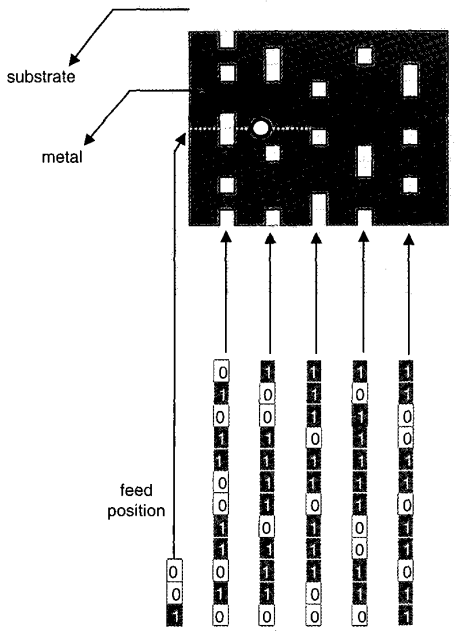

Fig. 9 *Encoding for the dual-band design*

at a frequency of 1 GHz. It is known that slots in the microstrip have the effect of lowering the resonance frequency [11]. Therefore we adopt a slot-encoding scheme, shown in Fig. 9 to encode each shape into a chromosome. Five equally spaced vertical lines are chosen in the patch area. These pre-selected lines are encoded into a binary chromosome, where ones denote metal and zeros denote non-metal. In addition, three more bits are added to the chromosome to represent the position of the feed along the dashed line on the patch. Since significant power dissipation is expected due to the introduction of the slots, we account for the metal loss by adding the second term in the cost function:

$$Cost = \frac{1}{N}\sum_{n=1}^{N}(P_n + Q_n) \tag{2}$$

where

$$P_n = \begin{cases} S_{11}(\text{dB}) + 10\,\text{dB} & \text{if } S_{11}(\text{dB}) \geq -10\,\text{dB} \\ 0 & \text{if } S_{11}(\text{dB}) < -10\,\text{dB} \end{cases}$$

$$Q_n = \begin{cases} P_J(\text{dB}) + 70\,\text{dB} & \text{if } P_J(\text{dB}) \geq -30\,\text{dB} \\ 0 & \text{if } P_J(\text{dB}) < -30\,\text{dB} \end{cases}$$

$$P_J = \frac{R_s}{2}\int_s |J_s|^2 ds(\text{dB})$$

$$R_s = \sqrt{\frac{w\mu}{2\sigma}}$$

The first part of the cost function accounts for the impedance mismatch, in the same way as in (1). The second part of the cost function accounts for the metal loss generated by the current flowing on the patch. The conductivity of aluminum ($\sigma = 3.82 \times 10^7$ S/m) is used.

4.2 Simulation and measurement results

Fig. 10 shows the GA-optimised microstrip for dual-band operation. The white dot shows the position of the feed, which resides 12.5 mm from the left edge. Fig. 11 shows the

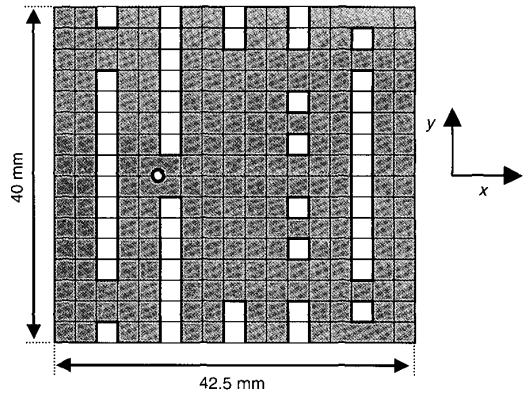

Fig. 10 *GA-optimised slot shape for dual-band operation*

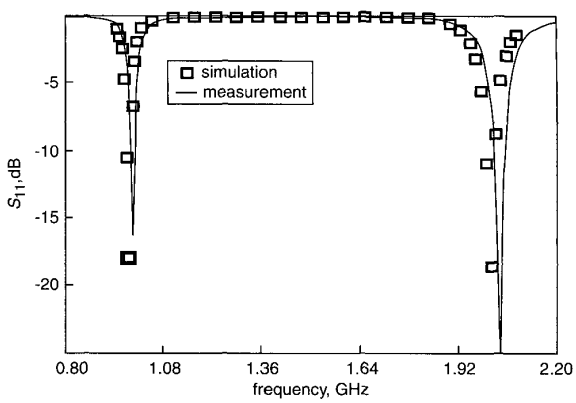

Fig. 11 *Return loss (dB) of the GA-optimised antenna from simulation and measurement*

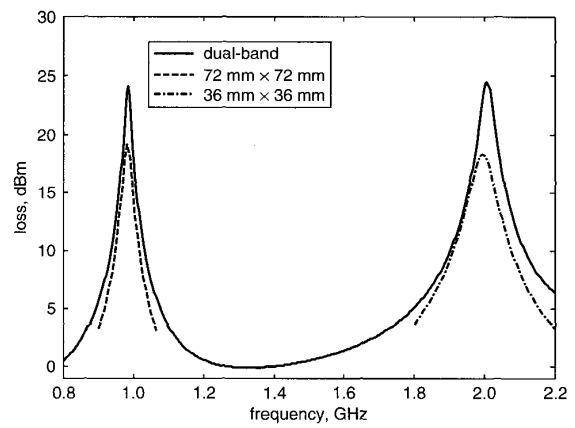

Fig. 12 *Simulated total metal loss (dBm) of the GA-optimised dual-band microstrip, a square microstrip of 72 mm × 72 mm and a square microstrip of 36 mm × 36 mm*

measurement and the simulation results of the return loss. Other than a slight shift in the resonant frequencies, the graph shows good agreement between the measurement and the simulation. The bandwidths at the two frequencies of 1 and 2 GHz are 1.2% and 1.37%, respectively. The measured relative gain of this microstrip shows a gain loss of −7 dB at 1 GHz and −7.5 dB at 2 GHz when compared to square microstrips operating at these two frequencies. To explain the gain loss, Fig. 12 shows the calculated metal loss (dBm) of the microstrips. The solid line is the metal loss of

the GA-designed microstrip, and the dashed lines are those of the reference square microstrips. At the low-band frequency (1 GHz), the GA-optimised microstrip shows a higher metal loss of 5 dB than the square microstrip of size 72 mm × 72 mm, while at the high-band it shows a 6 dB higher metal loss than the square microstrip of size 36 mm × 36 mm. These values show that the main cause for the gain loss comes from metal loss. It is noted that we have also optimised the dual-band microstrip without any constraint on the metal loss, and the resulting design shows an even larger metal loss. Thus the GA design achieves better radiation efficiency by taking the metal loss on the patch into consideration.

4.3 Operating principle of the GA design

To explain the miniaturisation principle of the GA design, we first note that a microstrip of size 42.5 mm × 40 mm without any slots has a resonant frequency of 1.7 GHz for the TM_{10} mode, and a resonant frequency of 3.4 GHz for the TM_{20} mode. Fig. 13 shows the current plots for the GA-optimised microstrip with slots at the resonant frequencies of 1 and 2 GHz. At the low band, the surface current distribution resembles the TM_{10} mode. The excited surface current is forced through the narrow channel that is near the feed. Since the current path is strongly meandered, the total length of the current path is increased. Therefore, the resonant frequency is reduced by a factor of about 1.7 compared to the microstrip without slots. At the high frequency band, the patch current resembles the TM_{20} mode. The currents are meandered around the two large vertical slots near two vertical radiating edges on the patch. In contrast to the slots near the feed, these slots lower the resonant frequency for the high band. We have verified

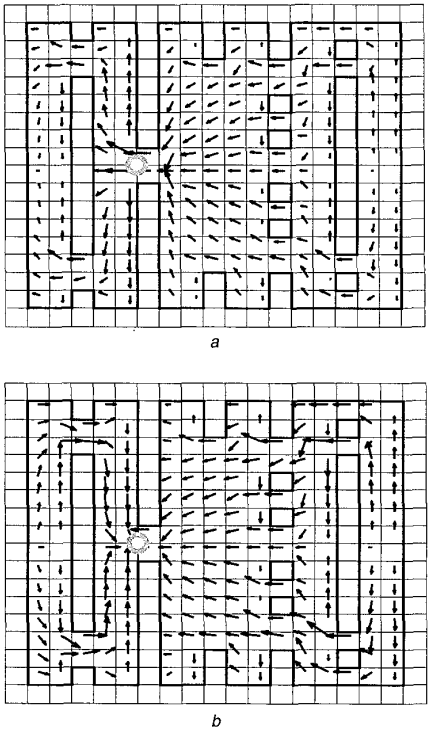

Fig. 13 *Current distribution on the surface of the GA-optimised patchs*
a At 1 GHz
b At 2 GHz

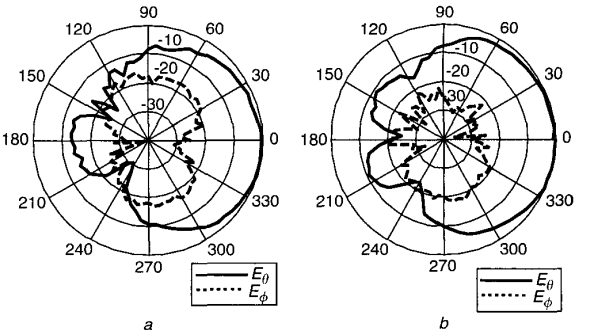

Fig. 14 *Measured radiation patterns*
a At 1 GHz ($\phi = 0$ plane)
b At 2 GHz ($\phi = 0$ plane)

these two effects through numerical simulation. If we slightly reduce the length of the large slots near the two radiating edges, we observe that the resonant frequency of the high band is increased. If we reduce the length of the slots near the feed, the resonant frequency of the low band is increased. These results clearly show that the miniaturization of the GA-optimised design is achieved by the frequency lowering effect of the slots to both the low and high frequency bands of the microstrip. Figs. 14*a* and 14*b* illustrate the measured radiation patterns at frequencies of 1 and 2 GHz, respectively. The radiation plots exhibit broadside radiation, and show less than a −20 dB cross polarisation level at both frequencies. In addition, the radiation patterns are almost identical at the two frequencies.

5 Conclusion

Optimised patch shapes for both broadband and dual-band microstrip antennas on a thin FR-4 substrate have been investigated using a genetic algorithm. For the broadband design, the optimised shape showed a four-fold improvement in bandwidth compared to a standard square microstrip. This result has been verified by laboratory measurement. The basic operating principle of the optimised shape can be explained in terms of a combination of two-mode operation and ragged edge shape.

For the dual-band design, the optimised shape showed good operation for both frequencies, with a 40% reduction in size as compared to a standard microstrip. The measurement result matched well with the numerical prediction. The operating principle of the optimised dual-band microstrip can be explained by the frequency-lowering effect from the narrow slots for the different modes operating at the two frequency bands. The gain loss due to the presence of the slots, however, is intrinsic to the miniaturised design. It is only partially alleviated by the GA process. Work on applying the GA approach to the design of a dual-band microstrip with arbitrary frequency spacing between the two bands can be found in [12].

Finally, the number of iterations needed for a GA to converge is, in general, quite large in our implementation. This results in a long computation time during the design. The convergence rate could potentially be reduced by hybridising the GA with other optimisation algorithms such as local search [13, 14] or Tabu search [15].

6 Acknowledgments

This work is supported by the Office of Naval Research under Contract N00014-01-0234, and in part by the Air

Force MURI Center for Computational Electromagnetics under Contract AFOSR F49620-96-1-0025. The authors would like to thank L. Trintinalia for providing the microstrip antenna software and A. Hutani for his help in the experimental set up.

7 References

1 JAMES, J.R., and HALL, P.S.: 'Handbook of microstrip antennas' (Peter Peregrinus, London, 1989)
2 POZAR, D., and SCHAUBERT, D.H.: 'Microstrip antennas' (IEEE, New York, 1995)
3 RAHMAT-SAMII, Y., and MICHIELSSEN, E.: 'Electromagnetic optimization by genetic algorithms' (John Wiley & Sons, New York, 1999)
4 ALATAN, L., AKSUN, M.I., LEBLEBICIOGLU, K., and BIRAND, M.T.: 'Use of computationally efficient method of moments in the optimization of printed antennas', *IEEE Trans. Antennas Propag.*, 1999, **47**, pp. 725–732
5 JOHNSON, J.M., and RAHMAT-SAMII, Y.: 'Genetic algorithms and method of moments (GA/MOM) for the design of integrated antennas', *IEEE Trans. Antennas Propag.*, 1999, **47**, pp. 1606–1614
6 CHOO, H., HUTANI, A., TRINTINALIA, L.C., and LING, H.: 'Shape optimization of broadband microstrip antennas using the genetic algorithm', *Electron. Lett.*, 2000, **36**, pp. 2057–2058
7 TRINTINALIA, L.C.: 'Electromagnetic scattering from frequency selective surfaces'. M.S. Thesis, Escola Politécnica da Univ. de São Paulo, Brazil 1992
8 CWIK, T., and MITTRA, R.: 'Scattering from a periodic array of free-standing arbitrarily shaped perfectly conducting or resistive patches', *IEEE Trans. Antennas Propag.*, 1987, **35**, pp. 1226–1234
9 DELABIE, C. VILLEGAS, M., and PICON, O.: 'Creation of new shapes for resonant microstrip structures by means of genetic algorithms', *Electron. Lett.*, 1997, **33**, pp. 1509–1510
10 ROSENFELD, A., and KAK, A.C.: 'Digital picture processing' (Academic Press, London, 1982, 2nd edn.)
11 GUO, Y.X., LUK, K.M., and LEE, K.F.: 'Dual-band slot-loaded short-circuited patch antenna', *Electron. Lett.*, 2000, **36**, pp. 289–291
12 CHOO, H., and LING, H.: 'Design of dual-band microstrip antennas using the genetic algorithm'. Proceedings of the 17th Annual Review of progress in applied comp. electromag. society, Monterey, CA, 2001, pp. 600–605
13 RENDERS, J-M., and FLASSE, S. P.: 'Hybrid methods using genetic- algorithm for global optimization', *IEEE Trans. Syst. Man Cybern.*, 1996, **26**, pp. 243–258
14 ZHOU, Y., LI, J.-M., and LING, H.: 'Reconstruction of cavity shapes using genetic algorithm combined with gradient search'. Proceedings of the 2002 International union for radio science meeting, San Antonio, TX, 2002, p. 399
15 GLOVEN, F., and LAGUNA, M.: 'Tabu search' (Kluwer Academic Publishers, Boston, 1997)